

Article

Enhancing Flame Retardancy: Enrichment of Huntite for Paint Industry Applications

Tülay Türk , Zeynep Üçerler * , İpek Sökmen and Murat Olgaç Kangal

Mineral Processing Engineering Department, Faculty of Mines, Istanbul Technical University, 34469 Istanbul, Turkey; turktu@itu.edu.tr (T.T.); sokmen17@itu.edu.tr (İ.S.); kangal@itu.edu.tr (M.O.K.)

* Correspondence: ucerler@itu.edu.tr

Abstract: Huntite, a naturally occurring carbonate mineral, originates through the alteration processes of dolomite and magnesite. While its structural characteristics align with typical carbonate minerals, its distinction arises from its polyhedral conjunctiveness. The versatile utility of huntite spans several industries, including paint, flame retardant, plastic, polymer, and pharmaceutical sectors. Noteworthy among its diverse applications is its utilization as a flame-retardant additive in raw materials. In this investigation, three samples received from the Denizli region of Turkey were subjected to detailed analysis followed by an enrichment process involving mechanical attrition and sieving of 38 microns where undersize products were obtained, exhibiting 86.9% huntite for the H-1 sample and 91.9% huntite for the H-2–3 sample. The huntite concentrates were then incorporated into paint formulations with the objective of enhancing flame retardancy. A series of testing protocols were implemented to assess the quality of the resulting paints, ultimately yielding a fire-resistant paint formulation through utilizing the H-1 sample.

Keywords: huntite; enrichment; industrial mineral; flame retardant mineral; paint



Citation: Türk, T.; Üçerler, Z.; Sökmen, İ.; Kangal, M.O. Enhancing Flame Retardancy: Enrichment of Huntite for Paint Industry Applications. *Minerals* **2024**, *14*, 180. <https://doi.org/10.3390/min14020180>

Academic Editors: Janos Kristof and Sunil Kumar Tripathy

Received: 8 December 2023

Revised: 12 January 2024

Accepted: 2 February 2024

Published: 7 February 2024



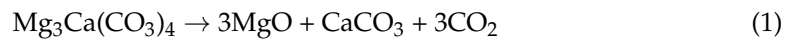
Copyright: © 2024 by the authors. Licensee MDPI, Basel, Switzerland. This article is an open access article distributed under the terms and conditions of the Creative Commons Attribution (CC BY) license (<https://creativecommons.org/licenses/by/4.0/>).

1. Introduction

Huntite, a mineral classified within the carbonate class, is categorized within the dolomite group and comprises a calcium magnesium carbonate composition. Typically occurring in association with hydromagnesite and/or magnesite, huntite exhibits a dispersed, pure white appearance [1]. The chemical formula of the huntite mineral is expressed as $3\text{MgO}\cdot\text{CaO}\cdot 4\text{CO}_2$, $3\text{MgCO}_3\cdot\text{CaCO}_3$ or $\text{Mg}_3\text{Ca}(\text{CO}_3)_4$. This composition places huntite between dolomite and magnesite on the mineralogical spectrum. In varying geological settings, trace amounts of elements such as Si, Fe, Sr, Ba, Ti, B, Al, and Mn may be detected within the huntite structure. Huntite's formation typically arises from the surface weathering or alteration of rocks that contain huntite, dolomite, or magnesite. It is commonly observed within the hollow spaces of rocks rich in magnesite, in travertine deposits, as well as in caves and fault zones, where it precipitates in the form of exceptionally fine grains from cold groundwater sources [2].

The most important use of huntite ore is as a flame-retardant filler material due to its CO_2 content upon heating. In addition, it is used as a special binder and adhesive in paints, as a filler hardener in special types of tires and as a coating material in the paper industry [3]. Huntite is preferred because the hardness of the huntite mineral falls within the range of 1–2 on the Mohs scale, thus making it easy to process. Furthermore, its production proves to be economically more advantageous compared to alternative flame retardants. The flame-retardant effect of the huntite can be enhanced through blending with other flame retardants in specific proportions [4]. The commercially manufactured derivative of huntite is referred to as UltraCarb. Formulated from huntite–hydromagnesite raw materials, UltraCarb serves as an industrial product employed as a flame-retardant filler in polymers, including polyethylene (PE), polypropylene (PP), polyvinyl chloride

(PVC), and rubbers. Application of UltraCarb products, which incorporate huntite as a filler material, is particularly advantageous in polymers utilized in floor and belt conveyor applications. This imparts notable advantages such as heightened heat absorption, safeguarding polymers against rapid thermal degradation, and mitigates the risk of combustion [1]. Huntite undergoes a sequential, two-step decomposition process, wherein the release of carbon dioxide occurs within the temperature range of 450 °C to 800 °C. The initial phase involves the decomposition of huntite into magnesium oxide, followed by a subsequent decomposition resulting in the formation of carbon dioxide and calcium carbonate. Lastly, the decomposition of calcium carbonate into carbon dioxide and calcium oxide takes place in the latter stage of the process [5].



For industrial applications, huntite must adhere to specific criteria. For its use as a flame retardant, huntite is required to exhibit a composition characterized by 33%–35% MgO, 15%–17% CaO, and a loss on ignition falling within the range of 45%–50%. Additionally, the concentrations of Al₂O₃, Fe₂O₃, K₂O, SiO₂, and TiO₂ should not exceed 0.1%, 0.05%, 0.02%, 0.5%, and 0.01%, respectively [6].

Paints are chemical substances that are applied to various surfaces for decorative and/or protective purposes in various ways and leave a hard and thin film layer on the applied surface. Fillers which are used in paints are low-cost inorganic pigments. The particle size distribution of fillers is very important. Fillers with finer particle sizes increase the coverage and gloss of interior paints and reduce the drying time. Mineral fillers are defined according to DIN 55,943 (EN-coloring material terms and definitions). Industrial minerals used as fillers are inexpensive and have physical and physico-chemical properties that contribute significantly to the quality and performance of the paint [7]. Huntite, which is found in very fine sizes and has flame-retardant properties, is one of the industrial minerals that can be used in paint.

Combustion is the rapid oxidative process leading to energy release. The occurrence of fire, a consequence of the chemical interplay between combustible materials and atmospheric oxygen, results from intricate physical and chemical reactions. Essential to combustion is the presence of an oxidizer. When subjected to heat, pressure, or both, the oxidizer liberates oxygen from its structure, thereby ensuring the combustion of the fuel [8].

Some criteria have been developed and standards have been set to measure the performance of a flame-retardant application under different conditions. The glow wire test (ASTM D6194-10), limiting oxygen index test (ASTM D2863-10), cone calorimeter test (ASTM E1354-11, ISO 5660-1, ISO 5660-2) and UL-94 test (ASTM D635-10, ASTM D3801-10) are the main combustion tests [8]. The experimental procedure of UL-94 involves the application of an open flame, with variations in flame intensity contingent upon the classification—either 50 watts (20 mm high flame) or 500 watts (125 mm high flame). The ignition source is applied to the test specimen for a duration of 30 s in the case of the horizontal burning test (HB), twice for intervals of 10 s each in the vertical burn test (V), and five times for 5 s intervals in the 5V test, after which it is removed. Evaluation criteria encompass the duration of combustion and the assessment of the fragmentary disintegration of burning components, particularly in the context of V-tests. The test results are categorized as V2, V1, and V0, with V0 representing the highest level of flame retardancy and V2 indicating the least flame retardancy [9].

The objective of this research is to obtain an upgraded huntite concentrate with maximum efficiency using the mechanical scrubbing method for use as a flame-retardant filler in paint formulations.

2. Materials and Methods

The sample obtained from Denizli, Türkiye, consists of huntite ores of different contents (H-1, H-2, and H-3). The X-ray fluorescence (XRF) method was used to determine the chemical composition of the ores. Chemical and ignition loss analyses of the samples were carried out according to TS EN-2980 standard using a Panalytical Axios X-ray fluorescence spectrometer (Worcestershire, UK). The results of the XRF analysis are given in Table 1.

Table 1. Chemical content of the representative samples.

	SiO ₂	Al ₂ O ₃	Fe ₂ O ₃	TiO ₂	CaO	MgO	Na ₂ O	K ₂ O	LOI ¹
H-1	4.50	1.01	0.575	0.044	22.36	27.01	0.01	0.12	44.32
H-2	5.77	0.62	0.309	0.023	20.99	27.46	0.11	0.05	44.62
H-3	5.65	0.99	0.339	0.032	19.67	28.30	0.05	0.05	44.87

¹ LOI: Loss on ignition.

The determination of huntite content through chemical analysis relies on the assessment of the MgO/CaO ratio. A MgO/CaO ratio of 3 signifies a very good huntite content in the ore. Based on X-ray fluorescence (XRF) results, the MgO/CaO ratios for H-1, H-2, and H-3 samples were calculated as 1.21, 1.31, and 1.43, respectively. Nevertheless, the MgO/CaO ratios alone do not sufficiently substantiate the presence of huntite in the ores. Given the high levels of both CaO and MgO in the raw ore samples, the presence of huntite cannot be overlooked. In light of this, X-ray diffraction (XRD) analyses were conducted to elucidate the huntite content in enrichment studies.

X-ray diffraction (XRD) analyses were performed to determine the mineralogical content of the representative samples using a Cu X-ray-sourced Panalytical X’Pert Pro diffractometer (Worcestershire, UK). PDF4/Minerals ICDD database software was used for mineral identifications. The XRD analysis results of the samples are given in Figures 1–3.

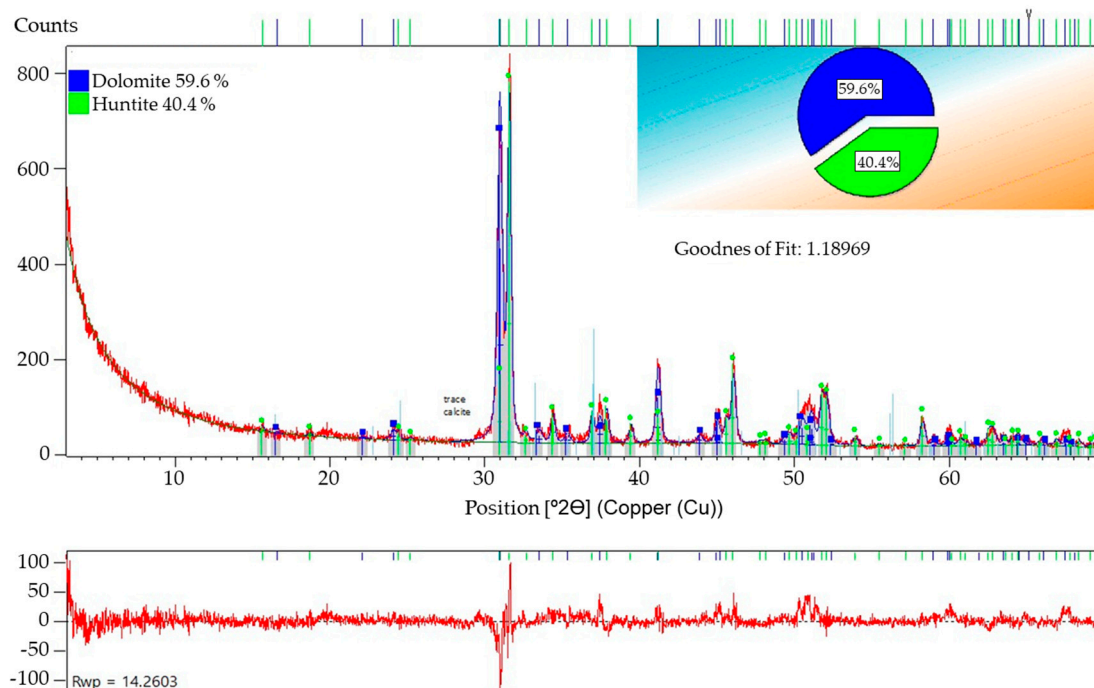


Figure 1. XRD analyses of H-1 sample.

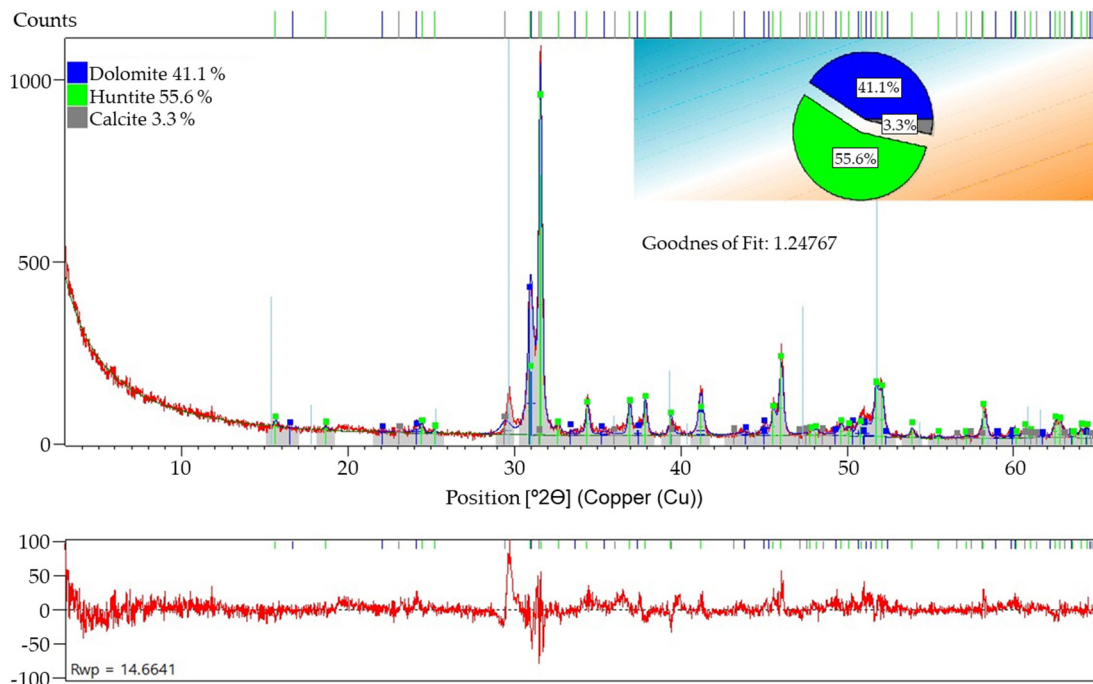


Figure 2. XRD analyses of H-2 sample.

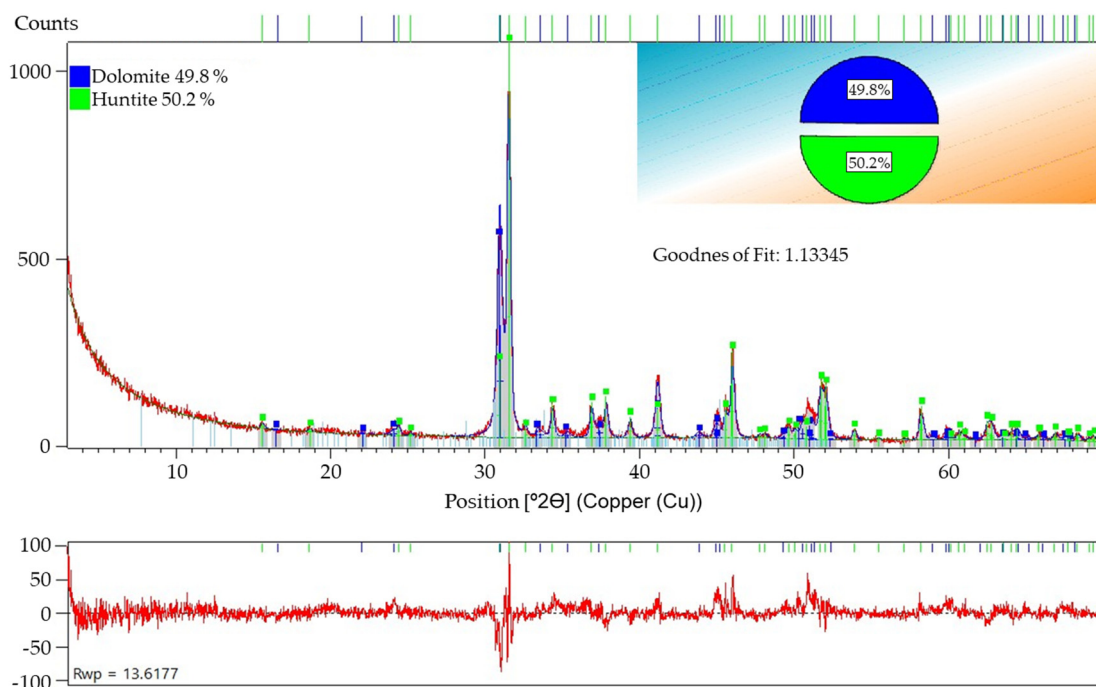


Figure 3. XRD analyses of H-3 sample.

According to the X-ray diffraction (XRD) analyses, the composition of the H-1 sample reveals 59.6% dolomite and 40.4% huntite. In the case of the H-2 sample, the analysis indicates 41.4% dolomite, 55.6% huntite, and 3.3% calcite. Likewise, the H-3 sample exhibits a composition of 49.8% dolomite and 50.2% huntite.

Differential thermal analysis (DTA) and thermogravimetric analysis (TGA) were performed on the different huntite ores using the STA 449 F3 Jupiter® thermal analyzer (NETZSCH, Selb, Germany). The DTA and TGA curves of huntite samples are given in Figures 4–6.

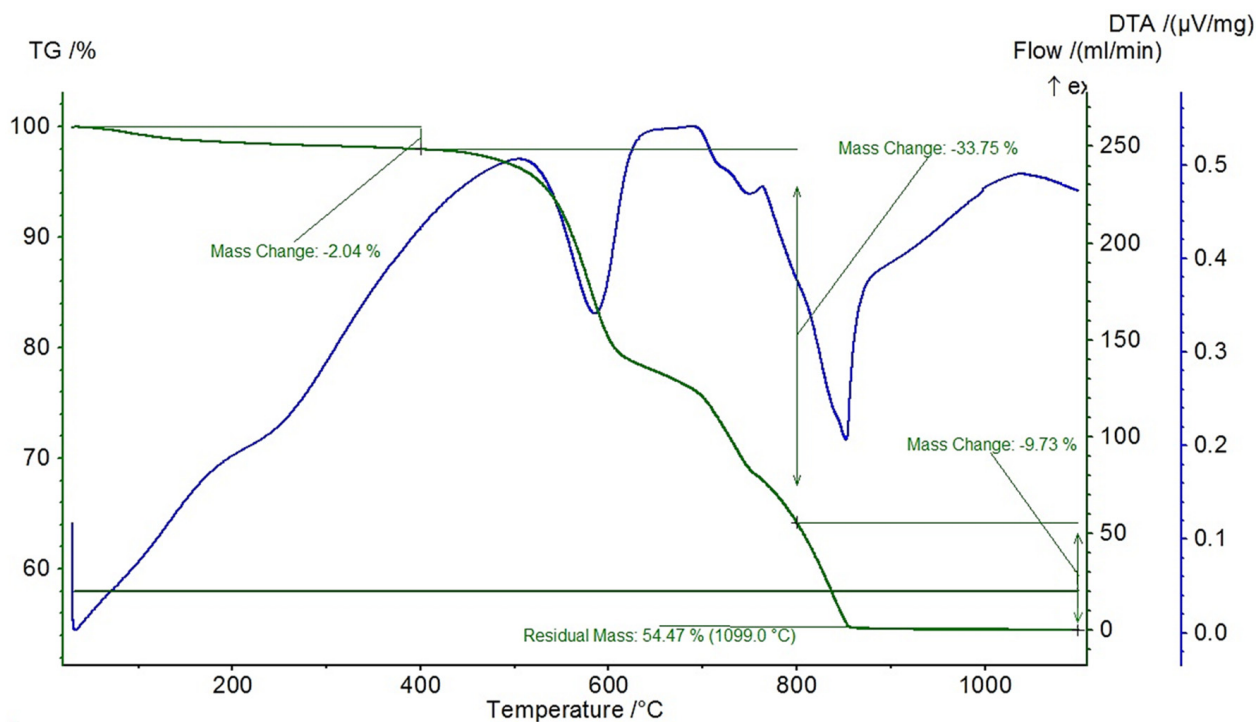


Figure 4. DTA-TGA analysis results of H-1 sample.

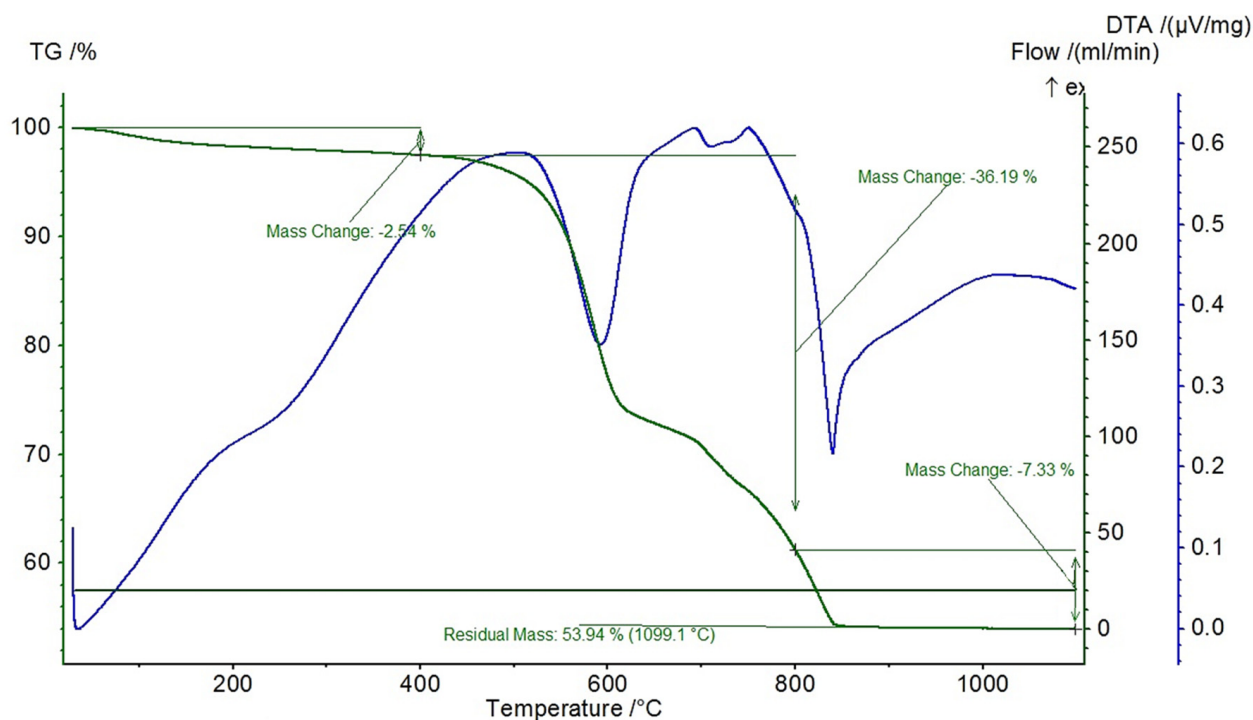


Figure 5. DTA-TGA analysis results of H-2 sample.

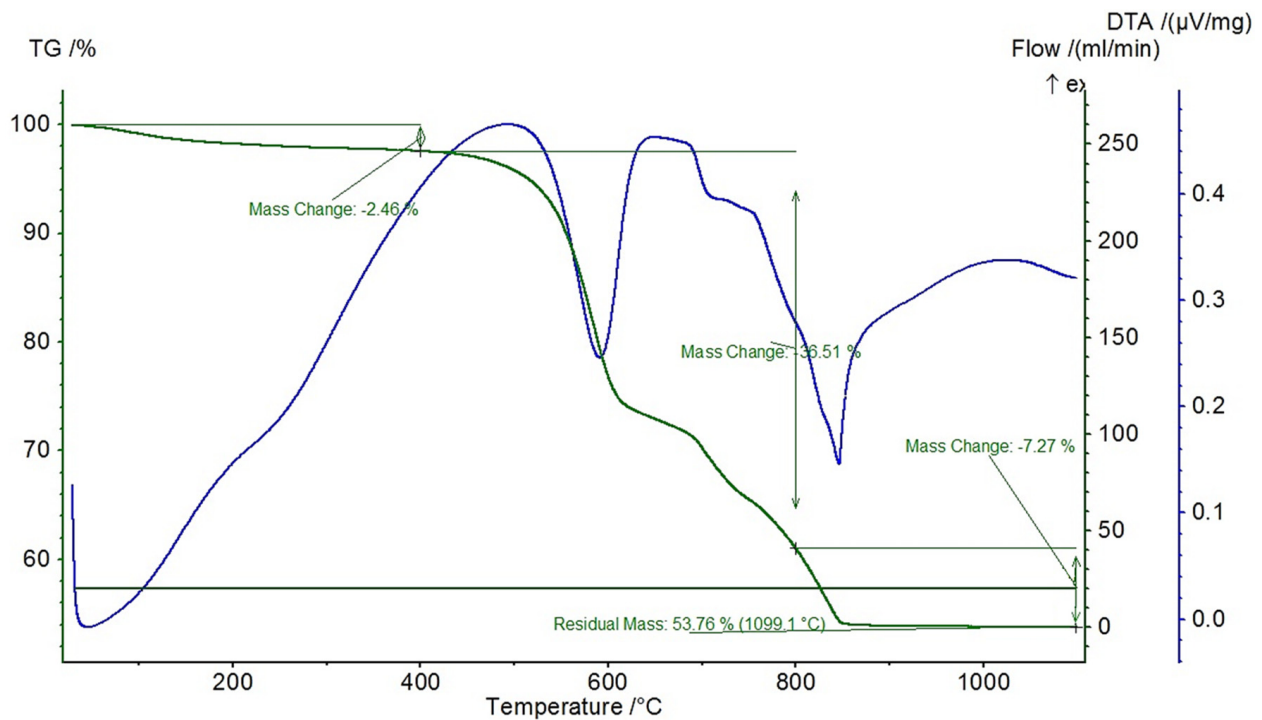


Figure 6. DTA-TGA analysis results of H-3 sample.

DTA-TGA investigation on the H-1 sample reveals a weight loss of 33.75% in the temperature range of 400–800 °C and a consequent loss of 9.73% between 800 and 850 °C. Similarly, the DTA-TGA analysis for the H-2 sample indicates a weight loss of 36.19% between 400 and 800 °C, and 7.33% between 800 and 830 °C. For the H-3 sample, the analysis demonstrates a weight loss of 36.51% between 400 and 800 °C, and 7.27% between 800 and 1000 °C. Notably, all the three samples exhibit a two-phase decomposition upon evaporation of water at low temperatures. Comparative DTA-TGA investigations involving pure huntite and dolomite reveal that while huntite undergoes decomposition at 500–600 °C, dolomite decomposes at 750 °C [10,11]. Huntite in the H-1 sample decomposes around 580 °C, and dolomite decomposes at approximately 850 °C. Likewise, in the H-2 and H-3 samples, huntite decomposition occurs at around 590 °C, with dolomite decomposition taking place at approximately 840 °C. The variation in the decomposition temperatures observed among the three ores can be attributed to the presence of impurities. Particularly, the absence of impurities in the reference samples (pure huntite and dolomite) made the observed differences acceptable.

Following the comprehensive characterization of the three huntite samples, and considering the similarity in content between H-2 and H-3 samples, enrichment experiments were conducted by mixing H-2 and H-3 samples. The enrichment process, which employed the scrubbing process, were performed separately for H-1 and mixed H-2–3 samples. The laboratory-scale FLSmidth Wemco attrition scrubber with the model number 52254 (Denmark) was utilized for the scrubbing experiments employing parameters such as mixing speed, mixing time, and solid ratio. After scrubbing, the samples were sieved from 38 microns. The final product, made under the optimal conditions, was subjected to an analysis through the XRD method to ascertain its huntite content prior to applying it in paint experiments.

The huntite concentrate, obtained with properties complying with fire retardant standards, was used in paint experiments. In the paint experiments, the 10% content of calcite filler in the water-based paint recipe was replaced with huntite. Three distinct paint samples were employed for the testing procedures: (i) 10% calcite (B0), (ii) 10% H-1 (B1), and (iii) 10% H-2–3 (B2). Water-based wall paint recipe was used during the experiments. The paints produced were subjected to viscosity measurements, color measurements, and zebra and burning tests. Lamy Rheology brand viscometer (Model: RM 200 Plus, Champagne-

au-Mont-d'Or, France) was used for the viscosity measurements. For the zebra test and color measurement test, measurements were made using zebra paper and the paint was applied on the zebra paper in one layer with a width of 6 cm. The coverage and color values of paint mixtures with different contents applied on zebra paper were measured using an X-Rite brand sphere benchtop spectrophotometer (Model: Ci7860, Michigan, US). The paint samples were applied to aluminum plates, ensuring a uniform paint thickness of 50 microns on each plate. Three combustion test specimens were prepared and attached to the stand in the fume hood. A vertical flame test was then conducted, applying a blowtorch at 1300 °C with a flame size of 20 mm directly to the plate.

3. Results

3.1. Mixing Speed Experiments

Table 1 presents the scrubbing test results of H-2 and H-3 samples which were combined due to their similar chemical contents. The mixing speeds in the range of 800–1200 RPM were studied at a constant 10% solid ratio for H-1 and H-2–3 samples. After the scrubbing, samples were sieved from a 38-micron screen. The results of the scrubber mixing speed experiments are given in Table 2 and Figure 7.

Table 2. Results of mixing speed experiments for H-1 and H-2–3.

Sample	Mixing Speed (rpm)	Products	Amount %	MgO		CaO		LOI	MgO/CaO Ratio
				C (%)	D (%)	C (%)	D (%)		
H-1	800	Oversize	46.67	25.31	40.06	15.77	34.85	42.05	1.60
		Undersize	53.33	33.13	59.94	25.80	65.15	45.00	1.28
		Total	100.00	29.48	100.00	21.12	100.00	43.62	1.40
	900	Oversize	44.54	24.45	37.58	26.1	58.73	45.03	0.94
		Undersize	55.46	32.62	62.42	16	44.83	44.67	2.04
		Total	100.00	28.98	100.00	19.80	100.00	44.83	1.46
	1000	Oversize	46.36	24.82	40.02	25.7	60.11	43.05	0.97
		Undersize	53.64	32.15	59.98	15.9	43.03	44.7	2.02
		Total	100.00	28.75	100.00	19.82	100.00	43.94	1.45
	1100	Oversize	45.46	24.6	38.69	26.1	59.24	44.14	0.94
		Undersize	54.54	32.5	61.31	16.2	44.11	45.03	2.01
		Total	100.00	28.91	100.00	20.03	100.00	44.63	1.44
	1200	Oversize	41.52	24.13	34.76	26.07	55.38	43.47	0.93
		Undersize	58.48	32.15	65.24	16.07	48.08	43.5	2.00
		Total	100.00	28.82	100.00	19.55	100.00	43.49	1.47
Mixed H-2–3	800	Oversize	17.2	26.96	14.9	23.00	21.9	45.20	1.17
		Undersize	82.8	31.93	85.1	17.05	78.1	42.79	1.87
		Total	100.0	31.07	100.0	18.07	100.0	43.20	1.72
	900	Oversize	19.1	27.31	16.7	22.61	24.0	43.18	1.21
		Undersize	80.9	32.19	83.3	17.05	76.7	45.41	1.89
		Total	100.0	31.26	100.0	17.98	100.0	44.98	1.74
	1000	Oversize	18.2	26.87	15.6	23.29	23.5	42.99	1.15
		Undersize	81.8	32.28	84.4	17.08	77.4	45.21	1.89
		Total	100.0	31.30	100.0	18.05	100.0	44.81	1.73
	1100	Oversize	15.1	27.31	13.1	24.12	20.2	43.35	1.13
		Undersize	84.9	32.19	86.9	17.1	80.6	45.23	1.88
		Total	100.0	31.45	100.0	18.02	100.0	44.95	1.75
	1200	Oversize	16.3	26.32	13.7	24.07	21.5	43.13	1.09
		Undersize	83.7	32.17	86.3	17.24	79.4	45.18	1.87
		Total	100.0	31.22	100.0	18.18	100.0	44.85	1.72

C: Content, D: Distribution, LOI: Loss on ignition.

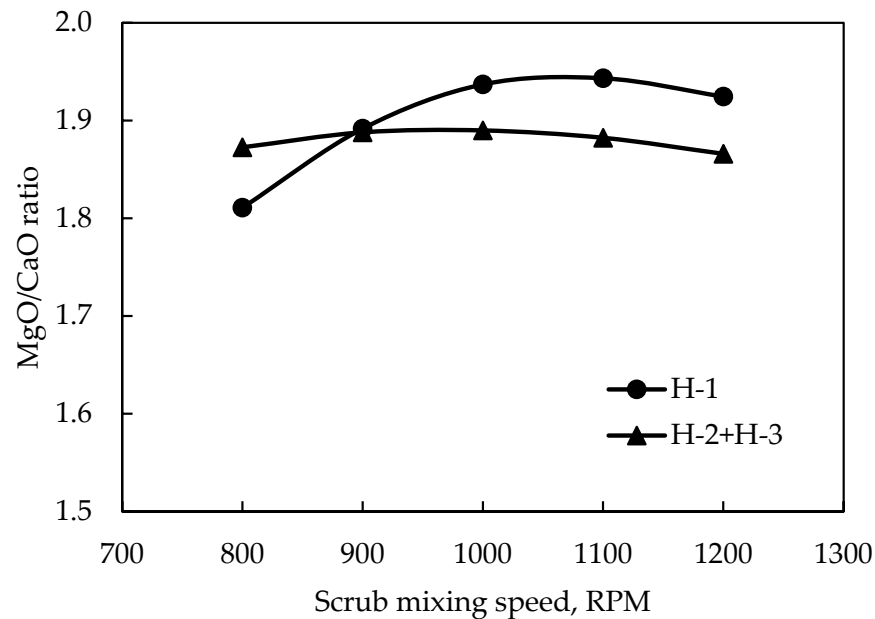


Figure 7. Results of mixing speed experiments for H-1 and H-2–3.

Huntite tends to predominantly accumulate in a finer-sized fraction of -38 microns primarily comprising huntite particles. The target huntite content in a sample relies on achieving a MgO/CaO ratio of 3. Scrubbing experiments revealed that, for the H-1 sample, the MgO/CaO ratio was notably low at 800 rpm but subsequently increased to 2 at 900 rpm, maintaining a similar ratio thereafter. In contrast, the H-2–3 sample exhibited a comparable trend across all mixing speeds, though with a marginally lower MgO/CaO ratio than the HS-1 sample. A mixing speed of 1000 RPM was chosen for both samples since H-1 reached the highest possible MgO/CaO ratio of 2.02 at 1000 RPM mixing speed, and H-2–3 samples have similar ratios at all mixing speeds. Optimizing the solid ratio in the pulp and adjusting mixing time parameters could augment the MgO/CaO ratio to the desired level of 3.

3.2. Mixing Time Experiments

The mixing speed was kept constant at 1000 RPM with 10% solid ratio for the mixing time which was varied in the range of 90–360 s; this was studied for H-1 and H-2–3 samples. In all the scrubbing experiments, the samples were sieved from 38 microns and analyzed separately. The results of the mixing time experiments are given in Table 3 and Figure 8.

As illustrated in Figure 8, the influence of mixing time on the MgO/CaO ratio appears to be insignificant for both H-1 and H-2–3 samples. Nonetheless, the H-2–3 sample consistently exhibits a slightly higher ratio across all mixing times compared to the H-1 sample. In light of the marginal difference between the two samples, a mixing time of 270 s was selected. This scrubbing duration resulted in MgO and CaO contents of 31.96% and 15.7%, respectively, for the H-1 sample, and 33.06% MgO and 15.99% CaO for the H-2–3 sample.

3.3. Solid Ratio Experiments

A mixing speed of 1000 RPM and mixing time of 270 s were kept constant for the solid content experiments in the scrubbing process. The 10%–20%–30% solid ratios were studied for the H-1 and H-2–3 samples. After the experiments, samples were sieved from 38 microns and analyzed separately. The results of the solid ratio experiments are given in Table 4 and Figure 9.

Table 3. Results of mixing time experiments for H-1 and H-2-3.

Sample	Mixing Time (seconds)	Products	Amount %	MgO		CaO		LOI	MgO/CaO Ratio
				C (%)	D (%)	C (%)	D (%)		
H-1	90	Oversize	42.77	22.78	34.87	24.89	54.09	44.08	0.92
		Undersize	57.23	31.80	65.13	15.79	45.91	45.21	2.01
		Total	100.00	27.94	100.00	19.68	100.00	89.29	1.42
	180	Oversize	44.91	24.26	38.41	25.87	59.37	44.28	0.94
		Undersize	55.09	31.71	61.59	15.64	44.02	45.77	2.03
		Total	100.00	28.36	100.00	19.57	100.00	90.05	1.45
	270	Oversize	43.69	23.87	36.69	25.84	58.13	44.24	0.92
		Undersize	56.31	31.96	63.31	15.7	45.53	45.55	2.04
		Total	100.00	28.43	100.00	19.42	100.00	89.79	1.46
	360	Oversize	43.57	23.68	36.55	25.56	57.67	44.28	0.93
		Undersize	56.43	31.74	63.45	15.71	45.91	45.53	2.02
		Total	100.00	28.23	100.00	19.31	100.00	89.81	1.46
Mixed H-2-3	90	Oversize	24.6	26.55	20.8	23.00	31.5	43.24	1.15
		Undersize	75.4	33.13	79.2	16.35	68.5	45.76	2.03
		Total	100.0	31.51	100.0	17.99	100.0	89.00	1.75
	180	Oversize	25.6	25.63	21.0	23.53	34.1	43.14	1.09
		Undersize	74.4	33.22	79.0	16.11	67.8	45.61	2.06
		Total	100.0	31.27	100.0	17.67	100.0	88.75	1.77
	270	Oversize	25.6	26.72	21.8	23.34	34.0	43.33	1.14
		Undersize	74.4	33.06	78.2	15.99	67.6	45.99	2.07
		Total	100.0	31.44	100.0	17.59	100.0	89.32	1.79
	360	Oversize	25.1	25.88	20.9	23.85	34.1	43.29	1.09
		Undersize	74.9	32.77	79.1	15.88	67.8	45.7	2.06
		Total	100.0	31.04	100.0	17.55	100.0	88.99	1.77

C: Content, D: Distribution, LOI: Loss on ignition.

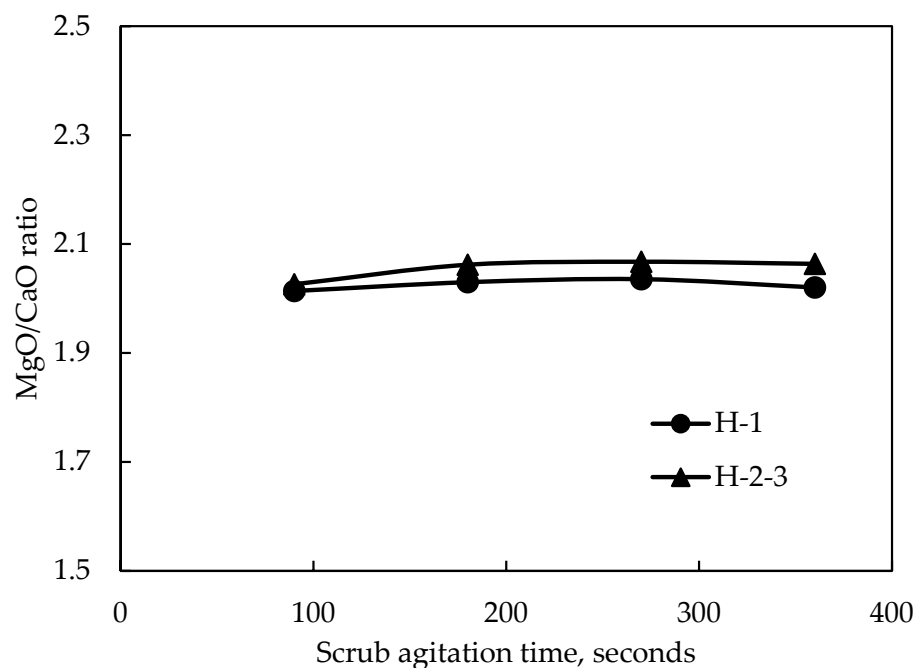


Figure 8. Results of mixing time experiments for H-1 and H-2-3.

Table 4. Results of solid ratio experiments for H-1 and H-2-3.

Sample	Solid Ratio (%)	Products	Amount %	MgO		CaO		LOI	MgO/CaO Ratio
				C (%)	D (%)	C (%)	D (%)		
H-1	10	Oversize	44.6	24.0	37.6	26.0	58.0	43.5	0.9
		Undersize	55.4	32.0	62.4	15.1	42.0	45.0	2.1
		Total	100.0	28.4	100.0	20.0	100.0	44.3	1.4
	20	Oversize	43.4	24.0	36.9	26.0	56.4	43.8	0.9
		Undersize	56.6	31.5	63.1	15.4	43.6	45.8	2.0
		Total	100.0	28.2	100.0	20.0	100.0	44.9	1.4
	30	Oversize	37.1	23.3	29.1	26.6	49.7	43.1	0.9
		Undersize	62.9	33.5	70.9	15.9	50.3	45.5	2.1
		Total	100.0	29.7	100.0	19.9	100.0	44.6	1.5
Mixed H-2-3	10	Oversize	25.3	26.5	21.5	23.9	33.0	43.1	1.1
		Undersize	74.7	32.7	78.5	16.4	67.0	45.6	2.0
		Total	100.0	31.2	100.0	18.3	100.0	44.9	1.7
	20	Oversize	23.0	25.3	19.9	24.8	32.6	43.3	1.0
		Undersize	77.0	30.5	80.1	15.3	67.4	45.2	2.0
		Total	100.0	29.3	100.0	17.5	100.0	44.8	1.7
	30	Oversize	20.5	23.3	14.8	26.6	31.5	44.4	0.9
		Undersize	79.5	34.5	85.2	14.9	68.5	45.4	2.3
		Total	100.0	32.2	100.0	17.3	100.0	45.2	1.9

C: Content, D: Distribution, LOI: Loss on ignition.

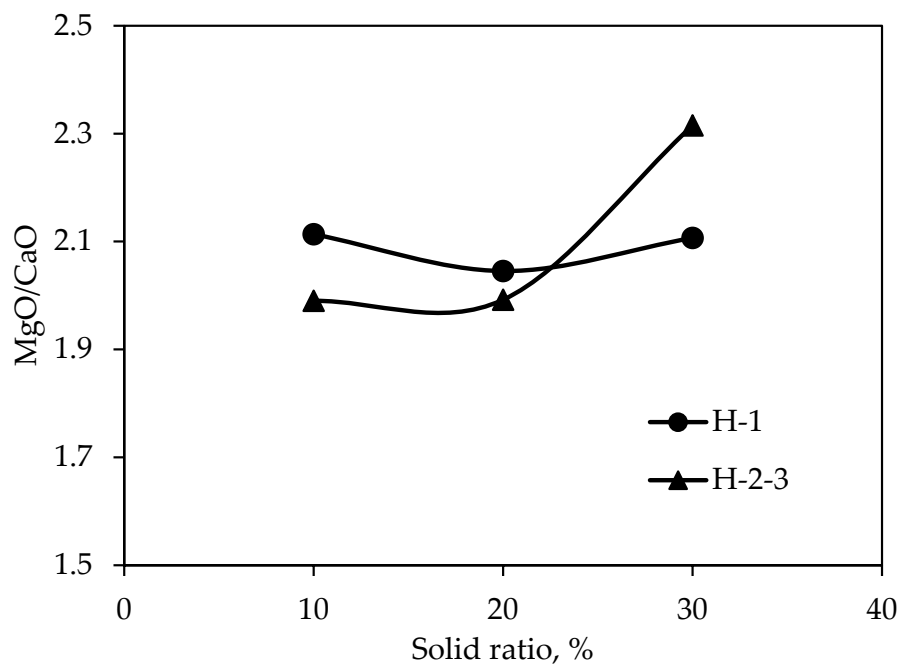


Figure 9. Results of solid ratio experiments for H-1 and H-2-3.

As a result of the solid ratio experiments, the H-1 sample indicated a similar trend in terms of MgO/CaO ratio; however, the H-2-3 sample yielded similar MgO/CaO ratios with different contents for 10% and 20% solid ratios (32.7% MgO and 16.4% CaO for 10% solid ratio, and 30.5% MgO and 15.3% CaO for 20% solid ratio). However, the H-2-3 sample showed a significant rise in terms of MgO/CaO ratio for the 30% solid ratio, resulting with 34.5% MgO and 14.9% CaO content, which was close to the specifications for flame-retardant minerals. Therefore, the 30% solid ratio was chosen for the optimum condition for the scrubbing solid ratio. After the chemical analysis, XRD and DTA-TGA analyses were performed to prove that concentrates consist of mostly huntite in their composition and they can be used

as a flame-retardant mineral in paint experiments. The results of the XRD analysis for the 30% solid ratio for H-1 and H-2-3 samples are given in Figures 10 and 11, and the DTA-TGA results for the 30% solid ratio for H-1 and H-2-3 samples are given in Figures 12 and 13.

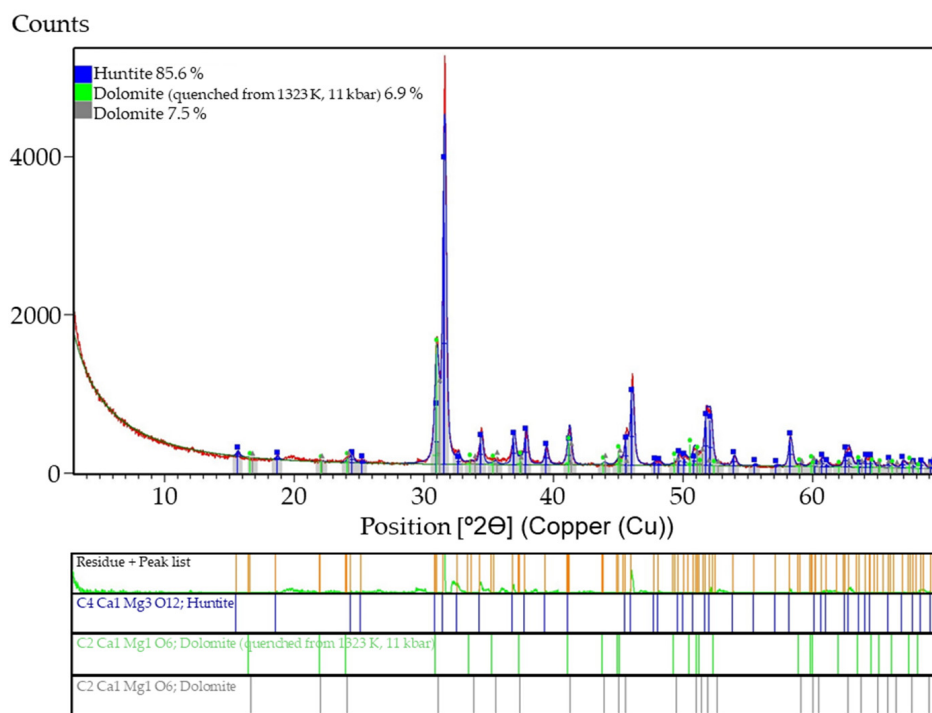


Figure 10. XRD analysis results of H-1 sample (30% solid ratio).

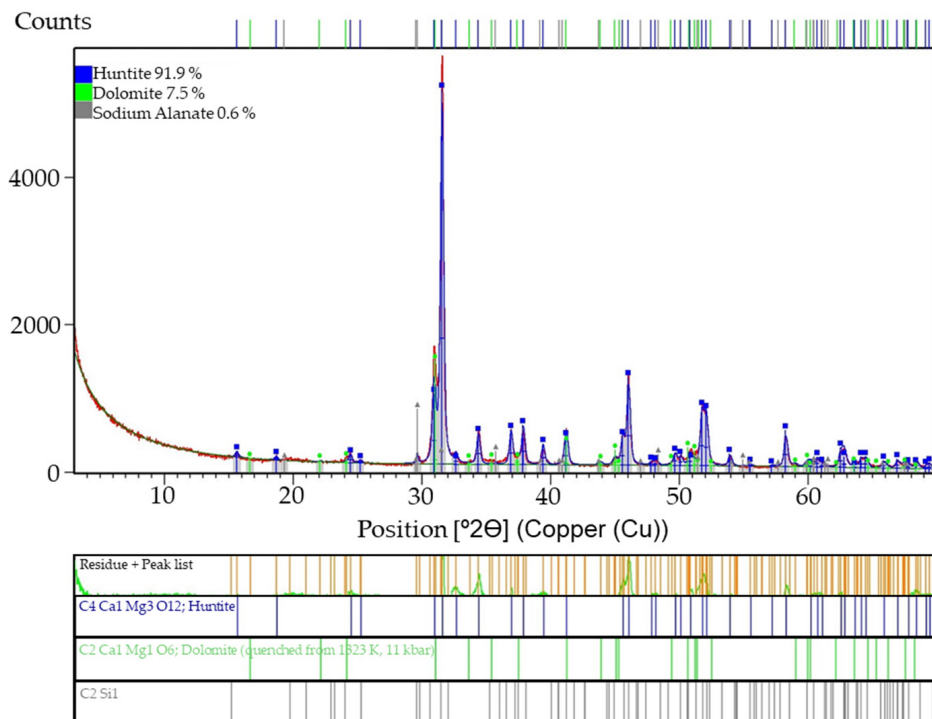


Figure 11. XRD analysis results of H-2-3 sample (30% solid ratio).

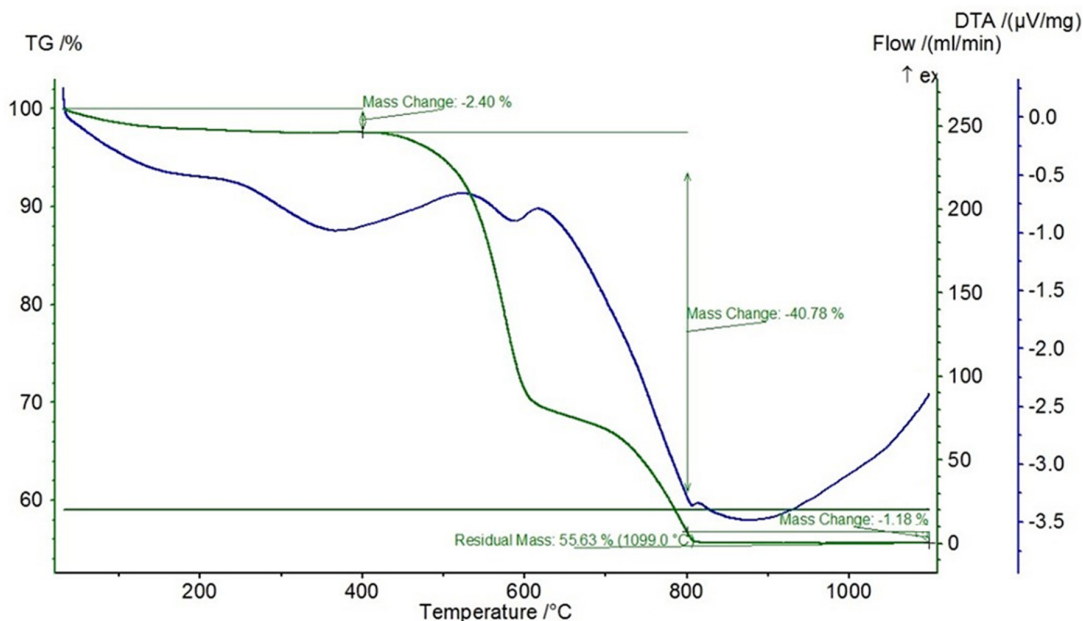


Figure 12. DTA-TGA analysis results of H-1 sample (30% solid ratio).

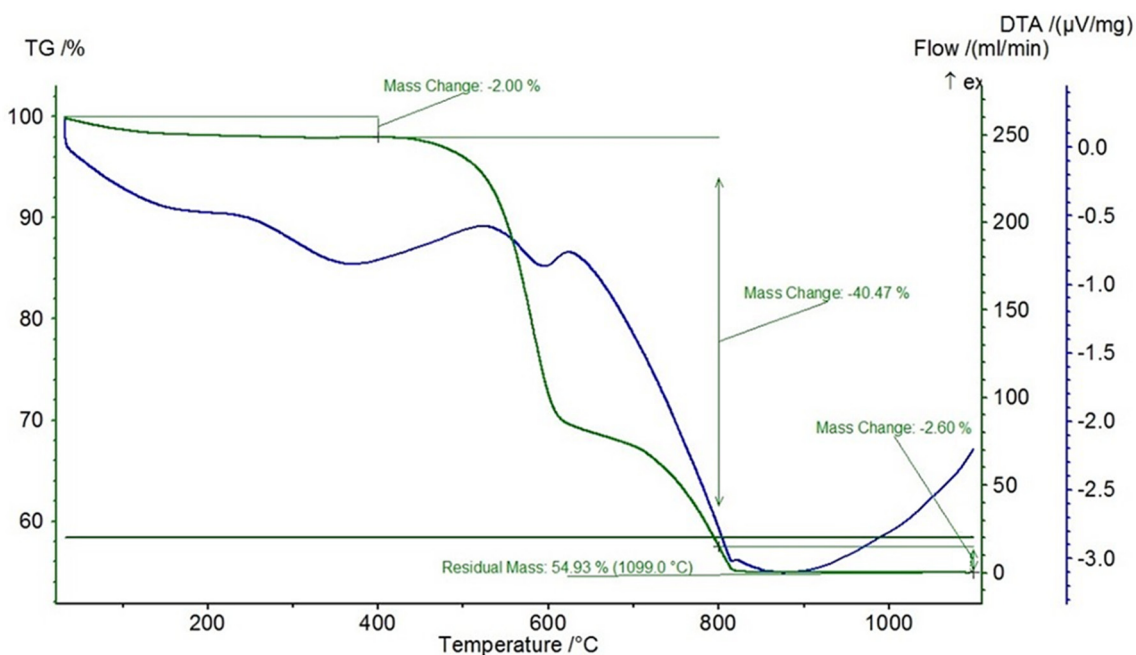


Figure 13. DTA-TGA analysis results of H-2-3 sample (30% solid ratio).

X-ray diffraction (XRD) analyses were conducted to characterize the undersized product resulting from the scrubbing process utilizing H-1 and H-2-3 samples under optimal conditions, i.e., a mixing speed of 1000 RPM, a mixing time of 270 s, and a solid ratio of 30%. The outcomes of the XRD analysis reveal that the H-1 sample comprises 86.9% huntite, 12.6% dolomite, 0.3% calcite, and 0.2% quartz. In contrast, the H-2-3 sample is composed of 91.9% huntite, 7.5% dolomite, and 0.6% sodium alanate.

The differential thermal analysis and thermogravimetric analysis (DTA-TGA) reveal that the undersized product of the H-1 sample, enriched with a solid ratio of 30%, exhibits a moisture loss at 55 °C, accounting for a weight reduction of 2.40%. Notably, the distinctive decomposition characteristics associated with huntite ores provide evidence that the first decomposition occurs at 600 °C, resulting in a weight loss of 40.78%, followed by a second decomposition at 800 °C, with a weight loss of 55.63%. The residual 1.8% weight is

completely lost at 1099 °C. Similarly, the undersized product of the H-2-3 sample, enriched with a 30% solid ratio, displays a moisture loss at 50 °C, corresponding to a 2% reduction in weight. The thermal decomposition profile reveals the occurrence of the first decomposition at 600 °C, with a weight loss of 40.47%, followed by a second decomposition at 800 °C, resulting in a weight loss of 54.93%. The remaining 2.60% weight is lost at 1099 °C.

3.4. Paint Experiments

Huntite concentrates (H-1 and H-2-3) obtained from the optimized enrichment tests were utilized in the production of water-based paint as a filler material instead of calcite at a rate of 10% by weight. The reference paint containing 10 wt% calcite was coded as B0, and paint formulas containing 10 wt% of H-1 and H-2-3 samples instead of calcite were coded as B1 and B2, respectively. After the production of paint, the samples were subjected to viscosity measurements, a color measurement test, zebra test and burning test. The results of viscosity measurements are given in Table 5, the results of zebra tests and color measurement tests are given in Figure 14 and Table 6, respectively, and the results of the burning test are given in Figure 15 and Table 7.

Table 5. The results of viscosity measurements of B0, B1, and B2.

	B0 10% Calcite 0% Huntite	B1 10% H-1 Sample	B2 10% H-2-3 Sample
Measurement System	RV3	RV3	RV3
Temperature (°C)	30	30.11	28.8
Speed (RPM)	100	100	100
Time (seconds)	25	25	25
Torque (Nm)	1.848	1.868	1.540
Viscosity (Poises)	25.7	26.0	21.4

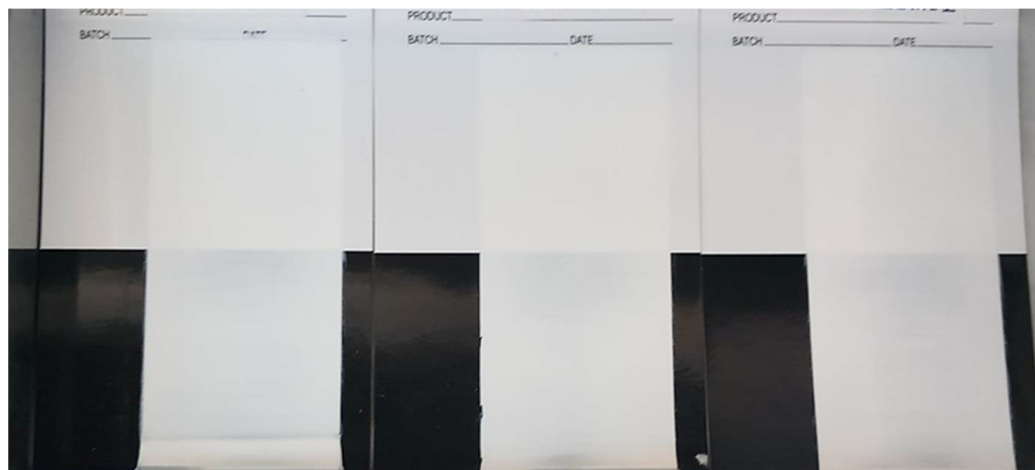


Figure 14. B0, B1, and B2 samples, respectively, applied on the zebra paper.

Table 6. Color measurement results of B0, B1, and B2 samples.

	L*	a*	b*	YI-E314	WI-CIE	Opacity_CR	X	Y	Z
B0	94.7	−0.71	1.74	2.80	78.95	91.24	82.0	86.9	90.7
B1	94.5	−0.67	1.80	2.95	78.12	94.09	81.5	86.4	90.1
B2	94.6	−0.64	2.00	3.35	77.44	91.83	81.8	86.6	90.0

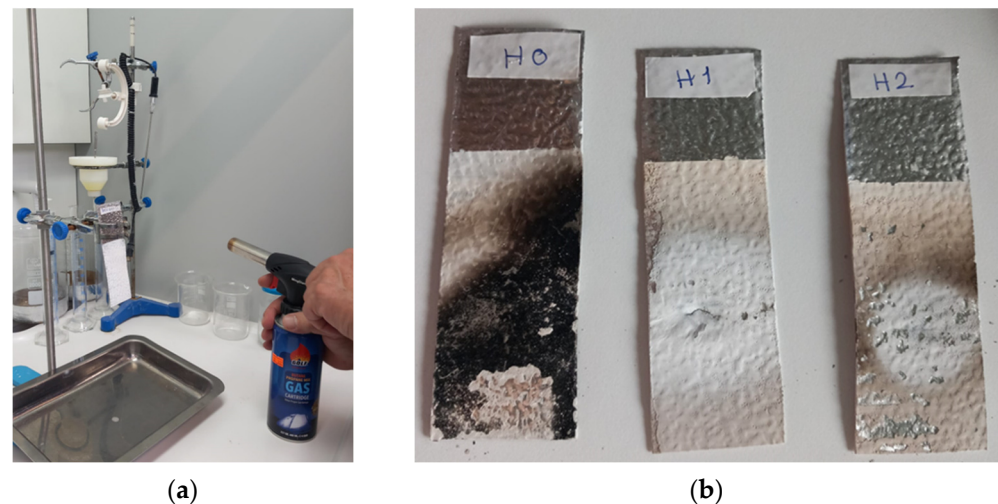


Figure 15. Burning test for B0, B1, and B2 samples. (a) Combustion apparatus; (b) burning test specimens after applying flame.

Table 7. Chemical content of the representative samples.

	Flame Exposure Time (s)	Ignition Time (s)	Extinguishing Time (s)	Dripping	UL-94 Classification
B0	10	4	7	None	V1
B1	30	No burning	No burning	None	V0
B2	30	15	2	None	V0

Based on the outcomes of the viscosity tests, both B0 and B1 samples exhibit comparable viscosity, while B2 demonstrates slightly lower viscosity compared to B0 and B1.

The CIE (Commission Internationale de l’Eclairage, translated as the International Commission on Illumination) Color Systems employ a triad of coordinates for the purpose of determining the specific location of a color within a designated color space. Color spaces are divided into three categories such as CIE XYZ, CIE L*a*b*, and CIE L*C*h°. The color index of zebra papers was assessed utilizing a spectrophotometer. The L* scale quantifies brightness, with L* values ranging from 0, representing black, to 100, indicating diffuse white. The a* scale denotes the degree of redness for positive values and greenness for negative values, while the b* scale represents the presence of yellow for positive values and blue for negative values [12]. The paint achieving the maximum opacity value demonstrates superior coverage, effectively concealing the dark surface of the zebra paper.

Upon conducting color measurements, it was observed that the brightness levels of all samples were notably similar, exhibiting high luminosity. The a* values for all samples were consistently negative, and similarly, the b* values were positive, indicating a prevalent green and yellow coloration across the samples. However, the a* and b* values recorded notably low values, signifying that the samples closely approach a white coloration according to the relevant color scale. In the context of opacity, B1 exhibited the highest value, signifying superior coverage, a trend visually apparent in Figure 14.

In the combustion tests, a flame was applied to the samples using a blowtorch at a temperature of 1300 °C for a duration of 10 s for the B0 sample. The sample ignited within 4 s and extinguished in 7 s. In contrast, the B2 sample, when subjected to a flame for 30 s, exhibited a prolonged ignition time of 15 s and a quicker extinguishing time of 2 s. As for the B1 sample, a flame was applied for 30 s, yet no combustion occurred. Notably, no dripping was observed for any of the samples. In this regard, B1 demonstrated the highest flame-retardant characteristics. Furthermore, both B1 and B2 samples can be classified as V0 according to the UL-94 classification system.

4. Conclusions

After determining the characteristics of the experiments with three different huntite ores from Denizli region, samples coded as H-2 and H-3 were blended and the optimum scrubbing conditions for H-1 and H-2–3 samples were determined as 1000 RPM mixing speed, 270 s mixing time and 30% solids in the pulp. Subsequent experiments under these conditions yielded huntite concentrates assaying 86.9% huntite for sample H-1 and 91.9% huntite for sample H-2–3. These concentrates were employed as substitutes for calcite in a water-based paint formulation, leading to the production of paints with varying filler compositions.

The paints were subjected to comprehensive testing involving viscosity, zebra, color measurement, and combustion assessments. Notably, B0 and B1 exhibited similar viscosity values, with B2 demonstrating marginally lower viscosity. Among B0, B1, and B2 samples, B1 demonstrated superior hiding power. The collective outcomes of the conducted experiments conclusively demonstrate the successful generation of huntite concentrates of high quality, establishing them as highly effective flame-retardant materials suitable for integration into paint formulations. Evaluation of combustion characteristics revealed that the B0 sample exhibited high combustibility, whereas the B1 sample demonstrated the highest flame retardancy. While sample B2 exhibited greater flammability than B1, it concurrently displayed a prolonged ignition time and shorter extinguishing time. Consequently, both samples B1 and B2 unequivocally meet the V0 classification according to UL-94 standards, indicating the highest level of flame retardancy achievable.

Author Contributions: All researchers conceived of and designed the experiments; T.T. and İ.S. performed the experiments and analyzed the data; T.T., Z.Ü., İ.S. and M.O.K. contributed to writing the paper. All authors have read and agreed to the published version of the manuscript.

Funding: This research was funded by the Istanbul Technical University Circulating Capital Enterprise R&D, Project ID: 43752, and analyses were carried out by ESAN.

Data Availability Statement: The data presented in this study is contained within the article.

Acknowledgments: The authors would like to express their sincere thanks and appreciation to Istanbul Technical University Circulating Capital Enterprise R&D for their financial support, and to ESAN for supporting the analyses.

Conflicts of Interest: The authors declare no conflicts of interest.

References

1. Yücel, M.B.; Gül, Ö. Huntite in The World and in Turkey. Mineral Research and Exploration General Directorate, Department of Feasibility Studies. 2017. Available online: <https://www.mta.gov.tr/v3.0/sayfalar/bilgi-merkezi/maden-serisi/Huntit.pdf> (accessed on 3 December 2023). (In Turkish)
2. Faust, G.T. *Huntite, CaMg₃(CO₃)₄, A New Mineral*; U. S. Geological Survey: Reston, VA, USA, 1953; pp. 4–23.
3. Kangal, M.O. Göller Bölgesi Huntit Cevherinin Zenginleştirilmesi ve Alev Geciktirici Hammadde Üretimine Yönelik Kullanılması. Master's Thesis, İstanbul Technical University, İstanbul, Türkiye, 2004; p. 158. (In Turkish)
4. Kanbur, Y.; Tayfun, Ü. Mechanical, physical and morphological properties of polypropylene/huntite composites. *Sak. Univ. J. Sci.* **2017**, *21*, 1045–1050.
5. Hollingbery, L.A.; Hullb, T.R. The thermal decomposition of huntite and hydromagnesite. *Thermochim. Acta* **2010**, *509*, 1–11. [[CrossRef](#)]
6. Kangal, O.; Güney, A. A new industrial mineral: Huntite and its recovery. *Miner. Eng.* **2006**, *19*, 376–378. [[CrossRef](#)]
7. Kızılkonca Duran, E. Determination of Physical, Anticorrosive and Antibacterial Effects of Nano Metal Oxide Additives to Paints and Coatings. Ph.D. Thesis, İstanbul Technical University, İstanbul, Türkiye, August 2020. (In Turkish)
8. Zakut, M. Effects of Huntite/Hydromagnesite on Capacity of Flame Retardancy, Mechanical and Physical Properties of Polypropylene. Master's Thesis, İstanbul Technical University, İstanbul, Türkiye, September 2012; pp. 7–32.
9. Spelsberg. Available online: <https://www.spelsberg.com/service/technical-information/technical-information/tests-and-test-methods-according-to-ul-underwriters-laboratories/> (accessed on 2 December 2023).
10. Shahraki, B.K.; Mehrabi, B.; Dabiri, R. Thermal behavior of Zefreh dolomite mine (Central Iran). *J. Min. Metall. B Metall.* **2009**, *45*, 35–44. [[CrossRef](#)]

11. Bolger, R. Flame Retardant Minerals. *Ind. Miner.* **1996**, *340*, 29–39.
12. X-Rite. *A Guide to Understanding Color: X-Rite Color Management Whitepaper*; X-Rite: Grand Rapids, MI, USA, 2016; p. 11.

Disclaimer/Publisher's Note: The statements, opinions and data contained in all publications are solely those of the individual author(s) and contributor(s) and not of MDPI and/or the editor(s). MDPI and/or the editor(s) disclaim responsibility for any injury to people or property resulting from any ideas, methods, instructions or products referred to in the content.